

The EC 14026 stars – VIII. PG 1336 – 018: a pulsating sdB star in an HW Vir-type eclipsing binary

D. Kilkenny,¹ D. O’Donoghue,¹ C. Koen,¹ A. E. Lynas-Gray² and F. van Wyk¹

¹South African Astronomical Observatory, PO Box 9, Observatory 7935, South Africa

²Department of Physics, University of Oxford, 1 Keble Road, Oxford OX12 3RH

Accepted 1997 December 9. Received 1997 December 1; in original form 1997 August 11

ABSTRACT

The sdB star PG 1336 – 018 is found to be a very short-period eclipsing binary system, remarkably similar to the previously unique system HW Vir. In addition, and unlike HW Vir, the sdB star in the PG 1336 system shows rapid oscillations of the type found in the recently discovered sdB pulsators, or EC 14026 stars. The orbital period, 0.101 0174 d, is one of the shortest known for a detached binary. Analysis of photoelectric and CCD photometry reveals pulsation periods near 184 and 141 s, with semi-amplitudes of ~ 0.01 and ~ 0.005 mag respectively. Both oscillations might have variable amplitude, and it is probable that other frequencies are present with amplitudes ~ 0.003 mag or less. The 184- and 141-s pulsations are in the range of periods predicted by models for hot horizontal-branch stars. Analysis of medium-dispersion spectrograms yields $T_{\text{eff}} = 33\,000 \pm 1000$ K and $\log g = 5.7 \pm 0.1$ for the sdB primary star, a radial velocity semi-amplitude $K_1 = 78 \pm 3$ km s⁻¹ and a system velocity $\gamma = 6 \pm 2$ km s⁻¹. Spectrograms from the IUE Final Archive give $T_{\text{eff}} = 33\,000 \pm 3000$ K and $E(B - V) = 0.05$ for $\log g = 6.0$ models. The derived angular radius leads to a distance of 710 ± 50 pc for the system, and an absolute magnitude for the sdB star of $+4.1 \pm 0.2$. A preliminary analysis of *U*, *V* and *R* light curves indicates the orbital inclination to be near 81° and the relative radii to be $r_1 = 0.19$ and $r_2 = 0.205$. Assuming the mass of the sdB primary to be $0.5 M_{\odot}$ leads to a mass ratio $q = 0.3$ for the system, and indicates that the secondary is a late-type dwarf of type $\sim M5$. As with HW Vir, it is necessary to invoke small limb-darkening coefficients and high albedos for the secondary star to obtain reasonable fits to the observed light curves.

Key words: binaries: eclipsing – stars: individual: PG 1336 – 018 – stars: oscillations – stars: variables: other.

1 INTRODUCTION

The Edinburgh–Cape (EC) blue object survey has been under way for almost a decade now. A detailed description of the survey and the photometric/spectroscopic results for almost a thousand stars in the first zone have recently been published by Stobie et al. (1997b) and Kilkenny et al. (1997b) respectively. One of the most exciting results from the survey has been the discovery of a new class of pulsating star – these have been called EC 14026 stars, after the prototype EC 14026 – 2647. They are sdB stars which pulsate with very short periods (typically ~ 2 to 3 min); they have at least two oscillation frequencies (in some cases,

many more) and surface temperatures near 35 000 K. Results for the first four of these objects to be discovered, EC 14026 – 2647, PB 8783, EC 10228 – 0905 and EC 20117 – 4014, have been published by, respectively, Kilkenny et al. (1997a, hereafter Paper I), Koen et al. (1997, hereafter Paper II), Stobie et al. (1997a, hereafter Paper III) and O’Donoghue et al. (1997, hereafter Paper IV). These four stars all have main-sequence companions of F or G spectral type, and it was originally thought that this might be a characteristic of the EC 14026 stars – related perhaps to their evolutionary history. However, examples have now been found which have no *detectable* companion (e.g. O’Donoghue et al. 1998b, hereafter Paper VI).

With the discovery of the first pulsator (Paper I) a search was started for similar objects, first among the EC subdwarfs, then among the brightest known southern subdwarfs, and finally among the northern subdwarfs using, in particular, the Palomar–Green (PG) survey (Green, Schmidt & Liebert 1986) and the hot subdwarf catalogue of Kilkenny, Heber & Drilling (1988) as sources. In each case, the search started with the brightest subdwarfs and worked towards fainter stars. These programmes are continuing and, at the time of writing, well over 300 stars have been tested and a total of 12 pulsators found. The EC 14026 stars are important, as they provide potential for examining the internal structure of hot subdwarfs via identification of pulsation modes and for the determination of the rate of evolution via secular frequency changes caused by radius/mean density changes. The discovery of new stars is necessary to extend the sample of stars for such analyses, to establish whether an ‘instability strip’ or preferred temperature zone for pulsation occurs, and to test the detected frequencies against pulsation models.

The PG survey has been a fruitful source of sdB stars, and it is planned to work systematically through at least the brightest of these from the northern hemisphere. Many of the PG subdwarfs south of $\delta \sim +15^\circ$ have already been examined using southern hemisphere telescopes and, not unnaturally, priority has been given to a number of stars noted as variable or possibly variable by other authors. The subject of this paper, PG 1336–018, was measured with Strömgren photometry by Wesemael et al. (1992) and found to have (along with a number of other stars) a rather high standard deviation in the y magnitude. Prophetically, Wesemael et al. noted that one of their programme stars was the eclipsing binary HW Vir (= BD – 7°3477), and that it was conceivable that other large- σ_y stars might also be photometric variables. In this paper, data are presented which show PG 1336–018 to be an eclipsing system remarkably similar to HW Vir (see Menzies & Marang 1986 and Wood, Zhang & Robinson 1993), with the startling addition that the sdB star in the PG 1336–018 system is also a rapid pulsator.

2 PHOTOMETRIC OBSERVATION

A short, cloud-infested ‘high-speed’ run of observations was obtained for PG 1336–018 on the night of 1996 May 18/19 using the University of Cape Town (UCT) CCD photometer on the 1-m telescope at the Sutherland site of the South African Astronomical Observatory (SAAO). The UCT CCD instrument (designed by DO’D; see O’Donoghue, Koen & Kilkenny 1996 for a brief description) operates in frame-transfer mode, so that it can deliver continuous 10-s integrations with no time loss between measurements. With pre-binning it is possible to work somewhat faster, if desirable. On-line reductions using DoPhot can be carried out at the observing rate or faster (in uncrowded fields at least) so that close to ‘real time’ reductions are often attainable. In addition, it is possible to select field stars as comparison stars and to derive differential magnitudes from the reduced data at the telescope.

The ‘white light’ (unfiltered) data from May 18/19 were obtained in poor conditions, but it was clear that rapid variability was present. On the next night, a white light run of ~ 5.2 h (18 750 s) confirmed the rapid variations and rendered the observer (almost) speechless by revealing beautiful eclipses. This run is illustrated in Fig. 1. Immediately obvious are the eclipses, occurring with a period very close to 0.1 d, the substantial reflection effect, indicative of a much cooler secondary star, and the rapid, small-amplitude variability in the out-of-eclipse light curve. There is even some evidence for frequency ‘beating’ – look particularly at the portion of light curve between about FJD = 0.42 and 0.46. Fig. 2 is an expanded portion of Fig. 1 to show the rapid variability on a better scale.

The rapid variations are almost certainly caused by pulsation of the hot sdB component of the system. The first four sdB pulsators discovered were found to have F- or G-type companions (but could be quite well-separated binaries; no eclipses or reflection effects have been detected). Detailed arguments for the sdB star being the source of the pulsational variations have been given in Papers I–IV, for example. Briefly, the variations are strongly evident at the

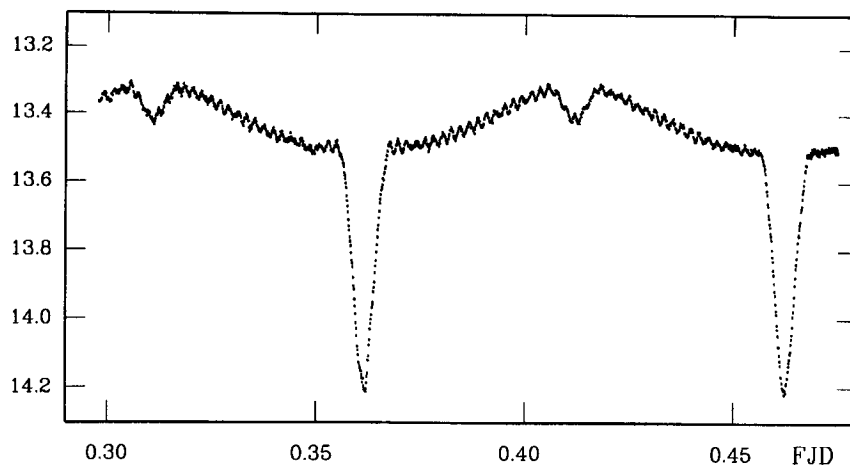


Figure 1. The ‘discovery’ light curve for the eclipsing nature of PG 1336–018 obtained with the SAAO 1-m telescope and UCT CCD photometer. The ordinate is a ‘white light’ magnitude with a zero-point such that the magnitude is roughly equal to a Johnson V . The abscissa is Fractional Julian Date (the data are from 1996 May 19/20; HJD 245 0223). The first part of the light curve (about an hour) has been omitted, as it was clearly affected by cloud.

bluer wavelengths (U and B), where the cool star contributes little to the total flux, and pulsation theory confirms that sdB stars would have low-order radial and non-radial modes with periods similar to those actually found; main-sequence F and G stars should not.

Although the eclipsing/pulsating nature of PG 1336 – 018 was discovered towards the end of the observing season for the object, we were able to obtain a few more short runs of data and these are listed in Table 1. The data were obtained mainly with the SAAO 1-m telescope and UCT CCD or St Andrews photometer (StAP); one run was obtained with the 0.5-m telescope and modular photometer. Johnson U , V and R filters were used in some runs, although the ‘white light’ mode is more usual for analysis of the pulsation frequencies (because the greater count rates give higher accuracy).

A referee has asked that some estimate be made of the precision of the photometric data sets. This is a non-trivial exercise because of the nature of the light curves, but we have made estimates by discarding the eclipse sections and removing the ‘reflection effect’ to a good approximation by fitting a sine wave to the out-of-eclipse data. The gross effects of pulsation were then removed by ‘pre-whitening’ the data by the two obvious frequencies found in the analysis described in Section 3. The data so modified then had rms values determined in groups of 20 data points. For the CCD data, typical rms values were ~ 0.004 to 0.007 mag; for the photometer data the values were ~ 0.01 to 0.02 mag, except for ‘ R ’ where the rms errors were typically 0.02 to 0.03 mag, reflecting the rather low count rates achieved through that filter. There are indications (see Section 3) that there might be more frequencies present in the sdB star

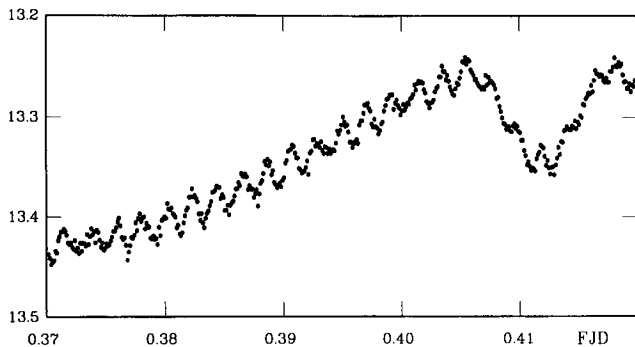


Figure 2. Part of the Fig. 1 light curve plotted on an expanded scale. Note that the pulsations are clearly present during secondary eclipse.

than the two we have removed, which means that the present estimates will not be a measure of purely random noise and could, therefore, be upper limits to the real photometric errors.

3 FREQUENCY ANALYSIS

For the frequency analysis, the data from each of the runs listed in Table 1 were reduced in the normal way (sky-subtraction and extinction correction, followed by differential magnitude correction in the case of the CCD data). Next, the eclipses were removed by simply discarding those data points, and the ‘reflection effect’ was removed to a good approximation by fitting a sine wave to the out-of-eclipse data. Periodograms were then determined for the data using the techniques of Deeming (1975), as modified by Kurtz (1985). The resulting periodograms are shown in Fig. 3 for the frequency range 2–10 mHz. At frequencies lower than 2 mHz (> 500 s), there is some power due to imperfect removal of the reflection effect and changes in the atmospheric extinction. If there are genuine pulsation frequencies with amplitudes comparable to those discussed below, and with frequencies lower than about 2 mHz, these will not be detectable with the present data sets.

From the periodograms in the range 2–10 mHz, the largest peak is found near 5.4 mHz (184 s) in each data set; this is also clear from Fig. 3. Removing this frequency from the data (‘pre-whitening’) and recomputing the periodograms results in the detection of the next highest frequency at 7.1 mHz (141 s) in four of the data sets. In the other four, this frequency is not unambiguously detected. The results from the periodogram analyses are listed in the final six columns of Table 1 (the two frequencies, f_1 and f_2 , together with the corresponding semi-amplitudes of the frequency fits and the periods, P_1 and P_2). From the Table 1 data, the mean values are $f_1 = 5.435 \pm 0.011$ and $f_2 = 7.076 \pm 0.011$ mHz, equivalent to $P_1 = 184.0 \pm 0.4$ and $P_2 = 141.3 \pm 0.2$ s.

Inspection of Fig. 3 suggests that the amplitudes of these pulsations are variable, although there is some uncertainty introduced by the use of different filters. Even so, the 141-s pulsation is clearly seen in four of the periodograms and is not detectable above the noise level in the other four. Note also that there appear to be differences in periodograms of runs made with the same equipment and filter combinations (e.g., the 141-s variation is clear in the first ‘white light’ run, but is not unambiguously detected in the second). That the variations might change amplitude is not particularly surprising, since the previously reported EC 14026 stars are

Table 1. Photometry of PG 1336 – 018.

Run	Date 1996	SAAO Tel	Phot	Length (hr)	Filter	f_1 (mHz)	s.amp. (mmag)	f_2 (mHz)	s.amp. (mmag)	P_1 (sec)	P_2 (sec)
dk049	May 19/20	1m	UCT CCD	5.2	-	5.433	0.011	7.062	0.005	184.1	141.6
dk054	May 20/21	1m	UCT CCD	5.0	-	5.437	0.011			183.9	
sdb104	May 26/27	0.5m	MP	2.0	CuSO ₄	5.415	0.018			184.7	
ck199	June 09/10	1m	StAP	2.7	U	5.426	0.008	7.080	0.005	184.3	141.3
ck221	June 10/11	1m	StAP	2.7	R	5.440	0.010			183.8	
ck222	June 10/11	1m	StAP	1.6	V	5.446	0.008			183.6	
m0252	June 17/18	1m	StAP	2.1	V	5.451	0.013	7.073	0.005	183.5	141.1
m0274	July 09/10	1m	StAP	2.9	V	5.434	0.011	7.089	0.005	184.0	141.1

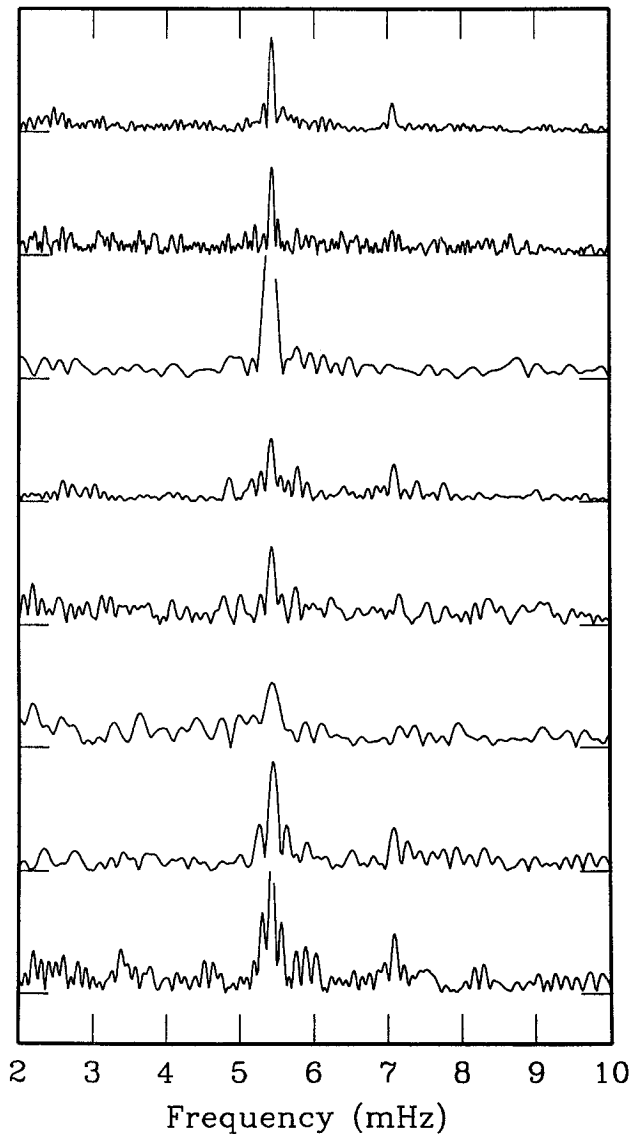


Figure 3. Amplitude spectra for the data from the eight runs listed in Table 1, ordered from top to bottom as in the table. The ordinate is semi-amplitude, the ordinate carets are separated by 0.015 mag, and the carets represent the zero of each plot. Note that there is evidence for variation near a frequency of 7.08 mHz in the first, fourth, seventh and eighth spectra (counting from the top) but not in the other four.

known to have short-term variation in pulsation amplitudes (e.g. Papers III and IV), and it has also been found that changes can occur on time-scales of a year or more. In this context, PB 8783, which had a very prominent pulsation in 1995 (Paper II) has been found to have a significantly smaller amplitude (though still detectable) pulsation in a recent multisite campaign (O'Donoghue et al. 1998a, hereafter Paper V).

In Fig. 4 the amplitude spectrum for run ck199 (1996 June 9/10) is shown, together with the window function derived from the same data set. The alias pattern in the window function is caused by the gaps where the eclipses were removed from the data set. Comparison of the upper and lower parts of Fig. 4 suggests that there might be real frequencies near 4.85, 5.75, 7.35 and 7.75 mHz with semi-

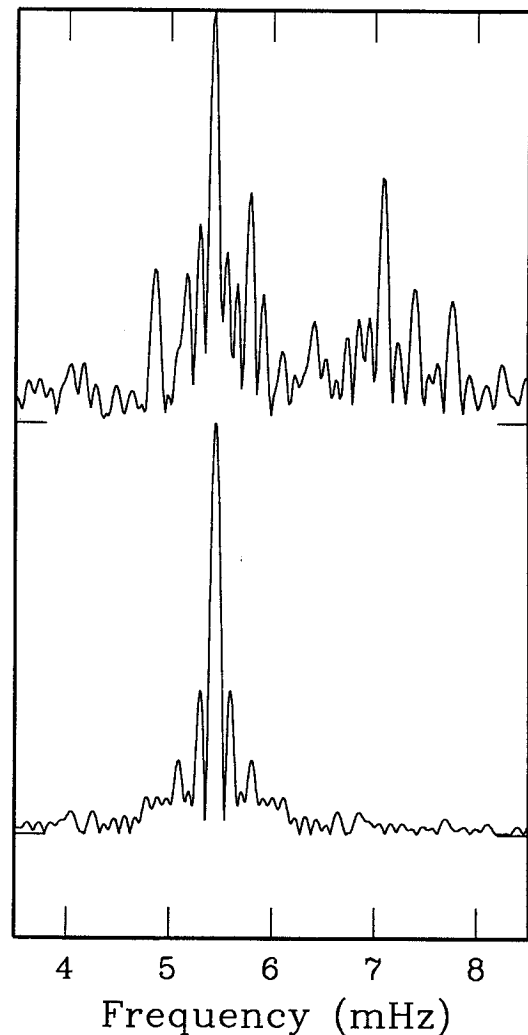


Figure 4. The upper part of the figure is the amplitude spectrum for data from the night of 1996 June 9/10, obtained with the SAO 1.0-m telescope, photoelectric photometer and a Johnson 'U' filter. The lower part is the spectral window for the same data set. Both spectra are normalized so that the main peak is the same size in each figure. In the case of the actual data the peak (semi-amplitude of the variation) is about 0.008 mag.

amplitudes ~ 0.003 mag, but apparently well above the background noise level. More extensive data will be required to check the reality of these.

The pulsations are clearly visible through secondary eclipse (see Figs 1 and 2), but what of primary eclipse? The primary eclipse data previously omitted from the frequency analyses were fitted with sine waves to remove the effect of the eclipses themselves (parabolic fits were tried, but were less satisfactory). Periodograms of the residual data do not show convincing evidence for the frequencies detected in the rest of the light curve, although the segments available for analysis are, of necessity, quite short. The residual data were also plotted together with a least-squares fit of f_1 and f_2 obtained outside eclipse, but again there was no really convincing match. However, the overall eclipse curves do not appear as smooth and symmetric as those of HW Vir (see, e.g., Wood et al. 1993), and it is quite possible that residual variations are present. Complete absence of variation in

primary eclipse would be a confirmation that the primary is the pulsator, but the eclipses are not total ($i=81^\circ$; see Section 7) so that, in principle, we could be seeing pulsations from either star. The fact that the pulsations seem completely undiminished during secondary eclipse, when most of the secondary star is obscured, is a strong argument in favour of the hot sdB star being the pulsator.

A recent report by Charpinet et al. (1998) describes sdB models in which the pulsation is driven by the κ -mechanism and an ‘opacity bump’ due to local enhancement of the iron abundance. A sample model with $T_{\text{eff}}=34\,000$ K and $\log g=5.8$ (very close to the surface characteristics determined for PG 1336 – 018 in Section 5) has p-mode radial pulsations with periods near to those actually seen in PG 1336 – 018. Similar values are also seen in the hot horizontal-branch models summarized in Paper III. Both sets of models also predict non-radial models ($\ell=1, 2, 3$) with frequencies close to the two frequencies unambiguously seen in PG 1336 – 018, and so it would be interesting to see if a longer and more complete data set could resolve any of these.

An interesting question arises from the fact that the pulsating star is describing an orbit in a plane close to the line of sight, namely, is it possible to detect any frequency change in the pulsation during the orbit? The data for two of the nights were fitted with sine waves at the frequency of the principal variation (f_1) in blocks of 110 data points (1100 s, or about six cycles). The data blocks overlapped each other by 50 per cent, and the phase difference for each block was determined, this being the most accurate way of searching for an orbit-related change. No significant effects were found. This is not surprising when it is realized that the orbit of the primary star is about 2.6×10^5 km in diameter (see Section 7), so that the light travel time across the orbit is only about 0.9 s, whereas the typical errors in the phase determinations for the short blocks of data were about 2 to 4 s. Furthermore, the frequency (f_2) will induce an apparent phase shift of the order of 14 s in size into the data, and f_2 itself might have a variable amplitude. It is concluded that the present data are not adequate to determine any such phase/frequency changes with the orbital motion. None the less, in principle this is a way to determine $a_1 \sin i$ directly; it will require precise data to allow detailed modelling of the pulsations.

4 THE EPHEMERIS

The determination of an accurate period for a system such as PG 1336 – 018 is important, not merely for phasing the photometric and spectroscopic data or providing an ephemeris for future observations, but because a binary with such a short period is likely to exhibit *detectable* secular period changes. HW Vir itself has been shown to have a decreasing period by Kilkenny, Marang & Menzies (1994). The cause of the changing period in HW Vir is not certain, but Kilkenny et al. (1994) have discussed the various possibilities and suggested that the most probable explanation is angular momentum loss due to magnetic braking in a weak stellar wind (see Patterson 1984). A mechanism such as this will have important consequences for the future evolution of the system. Furthermore, determination of rates of period change might give important clues to the origin of

these systems and possibly to the origin of the short-period cataclysmic binaries.

Following the procedures used for HW Vir (Kilkenny et al. 1994) the mid-points of primary eclipse have been measured using the bisected chords method. Two eclipses were omitted because they were too incomplete to give an accurate result; the remainder are listed in Table 2. The eclipse timings were then fitted with low-order polynomials using a program based on the POLFIT subroutine by Bevington (1969). The quadratic fit (implying a decreasing period) is better than the linear fit (see Table 2), but the baseline for the data is so short that it should not be considered significant at this stage. Table 2 includes an estimate of the error in the timing of the mid-point of each eclipse, but this estimate only allows for random errors in the bisected chord method; systematic errors – which might be caused by residual pulsations in the eclipses – could make these larger. (Note that the spread of residuals in, say, eclipses $E=0$ to 11 is 0.000 16 – about twice what would be expected from the timing errors alone.) Given that small departures from eclipse symmetry probably affect the eclipse timings at a similar level to the differences between the linear and quadratic fits, we prefer not to speculate on a non-linear ephemeris at present; one or two more seasons of observations should settle this question.

The linear fit results in an ephemeris:

$$T_{\text{min}} = \text{HJD } 245\,0223.361\,42 + 0.101\,0174E,$$

with formal errors of $\pm 0.000\,06$ and $\pm 0.000\,0003$ d in the zero-point and period respectively. Given the clear period change exhibited by HW Vir (Kilkenny et al. 1994), it would not be surprising to find the same in the closely similar (but slightly shorter period) PG 1336 – 018. The existence of this effect will certainly be eagerly sought in future seasons.

The period 0.101 0174 d makes PG 1336 – 018 one of the shortest period *detached* binary systems known (see, e.g., Ritter 1987).

5 SPECTROSCOPIC ANALYSIS

Spectroscopic observations of PG 1336 – 018 were made in 1996 May, June and July with the Image-Tube Spectrograph (ITS) and Reticon Photon-Counting System on the 1.9-m telescope at the Sutherland site of the SAAO. Grating 9 was used, and this gives a reciprocal linear dispersion of $\sim 30 \text{ \AA mm}^{-1}$ and a resolution of $\sim 1 \text{ \AA}$ in the blue. Stellar spectro-

Table 2. Primary eclipse timings of PG 1336 – 018.

E	HJD 2450000+	est. error	(O–C) (linear)	(O–C) (quadr.)	Filter
0	0223.36130	0.00004	–0.00017	–0.00009	-
1	0223.46243	0.00002	–0.00001	+0.00007	-
10	0224.37150	0.00003	–0.00010	–0.00003	-
11	0224.47255	0.00003	–0.00011	–0.00005	-
68	0230.23075	0.00002	+0.00016	+0.00014	CuSO ₄
207	0244.27216	0.00004	+0.00013	0.00000	U
217	0245.28236	0.00004	+0.00015	+0.00002	R
218	0245.38332	0.00005	+0.00010	–0.00003	V
286	0252.25248	0.00005	+0.00006	–0.00005	V
504	0274.27400	0.00007	–0.00021	+0.00002	V

grams were interspersed with Cu-Ar arc spectrograms, and reductions were carried out using an automated version of the *SKIP* reduction package, including cross-correlation for radial velocities. A summary of the observations is given in Table 3. The May and June data were obtained on single nights, and the July data over a week. The wavelength ranges listed in the table are the ranges used for the velocity cross-correlations. K_1 and γ , the semi-amplitude of the velocity variation and the systemic velocity, are discussed below. The final column gives the number of spectrograms measured.

Analyses of summed spectrograms were carried out following the fitting procedures described in Paper IV, except that in the case of PG 1336 subtraction of a companion of comparable brightness is not necessary. Fitting the Balmer line profiles, $H\gamma$ – $H9$ for the May/June data and $H\delta$ – $H9$ for the July data, results in $(T_{\text{eff}}, \log g) = (33\,139 \pm 1000 \text{ K}, 5.78 \pm 0.1)$ and $(32\,895 \pm 1000 \text{ K}, 5.67 \pm 0.1)$ respectively. The mean values $T_{\text{eff}} = 33\,000 \text{ K}$ and $\log g = 5.7$ are typical of the other sdB pulsators so far analysed.

The results from the cross-correlation analysis are summarized in Table 3, and plotted as individual data points in Fig. 5. The figure is disappointing because of the large scatter in the velocities. Examination of the table reveals that the May 23/24 data appear significantly different in radial velocity amplitude, and the June 17/18 data in systemic velocity. It does not appear likely that this is wholly a spectrograph stability problem, since reasonable velocity results have been obtained with the instrument (see, e.g., Lynas-Gray et al. 1986). Furthermore, the velocities from 1996

May appear to be systematically smaller, *in phase* with the other data, implying that the effect originates in the binary system. There is no evidence to indicate what this effect might be, but a possibility is variable, unresolved emission features from either gas in the system or the heated face of the secondary.

In 1996 July, HR 5107 (=HD 118098 = ζ Vir) was occasionally observed as a local ‘standard’. It is close to the position of PG 1336–018 and is of type A3Vn, not ideal for a velocity standard, but having relatively broad Balmer series lines which dominate the spectrum in the visible – very like an sdB star, and therefore (hopefully) indicative of the accuracy attained for the binary. Radial velocity results from July 16 to 19 were +7, +7, +6 and +4 km s^{-1} , indicating stability, although the published results for the radial velocity of HR 5107 cluster tightly around –13 km s^{-1} (Abt & Biggs 1972), so that there might be a ‘zero-point’ problem.

Given the problems noted above, we have not attempted to correct the data for PG 1336–018 to any other standard, and we would not want to rely on the velocities at better than the ~ 10 – 20 km s^{-1} level. Further observations for radial velocity measurement would certainly be advantageous.

6 IUE SPECTROPHOTOMETRY

PG 1336–018 was observed with the *IUE* satellite by Drs G. Fontaine and F. Wesemael on 1985 June 15. Low-resolution spectrograms (SWP26175 and LWP06224) were retrieved from the Final Archive, both images having been reduced following Nichols & Linsky (1996). The merged spectrograms are plotted in histogram form in Fig. 6, where the data are averaged into 10-Å bins. The use of *IUE* low-resolution spectra to constrain T_{eff} and $E(B-V)$ for the sdB star in the PG 1336–018 system followed the approach adopted in Paper VI, with small differences forced by the fact that PG 1336–018 is an eclipsing binary and the *IUE* spectra cannot (yet) be accurately phased with the light curve.

The ephemeris given in Section 4 predicts that the two *IUE* spectra, with mid-exposures at HJD 244 6232.302 07 (SWP) and 244 6232.333 28 (LWP) would fall at phases $\phi \sim 0.27$ and 0.58 respectively. The formal error in the ephemeris would change the times by only about 0.01 d over the $\sim 40\,000$ cycle gap between the *IUE* and optical data, corresponding to a phase difference of about 0.1, so that both spectra would probably be safely outside primary eclipse. However, since we have, as yet, no information on any non-linear effects in the ephemeris, and since these could be large over such a long baseline, it is necessary to consider circumstantial evidence.

The *IUE* spectra give flux densities in fair agreement in the region of overlap ($\sim 2000 \text{ \AA}$), suggesting they were obtained at roughly comparable phases; both are either unaffected by eclipses or equally affected. The latter is essentially impossible, as the exposure times (14 min for the SWP and 18 min for the LWP) are close to the total eclipse duration ($\sim 0.05\phi$) and the exposure separation is 0.0312 d, or 0.31 ϕ .

The out-of-eclipse variation is not insignificant (~ 10 per cent) and, in view of the uncertain phases of the *IUE* spec-

Table 3. 1996 spectroscopic observations of PG 1336–018.

Date 1996	λ range (Å)	K_1 km/s	γ km/s	n
May 23/24	3800–4400	47 ± 4	$+4 \pm 2$	24
Jun 17/18	3800–4400	74 ± 5	-8 ± 4	12
Jul 16–19	3750–4150	79 ± 4	$+9 \pm 3$	32
Jul 20–22	3850–4400	76 ± 8	$+12 \pm 6$	24

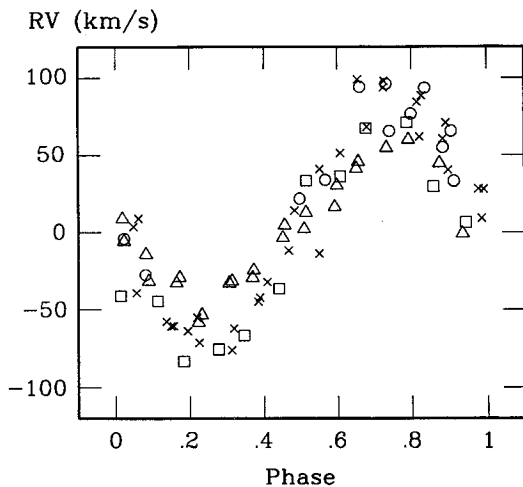


Figure 5. Radial velocity curve for the sdB primary in PG 1336–018. Symbols represent data from 1996 May (triangles), June (squares), July 16–20 (crosses) and July 20–22 (circles).

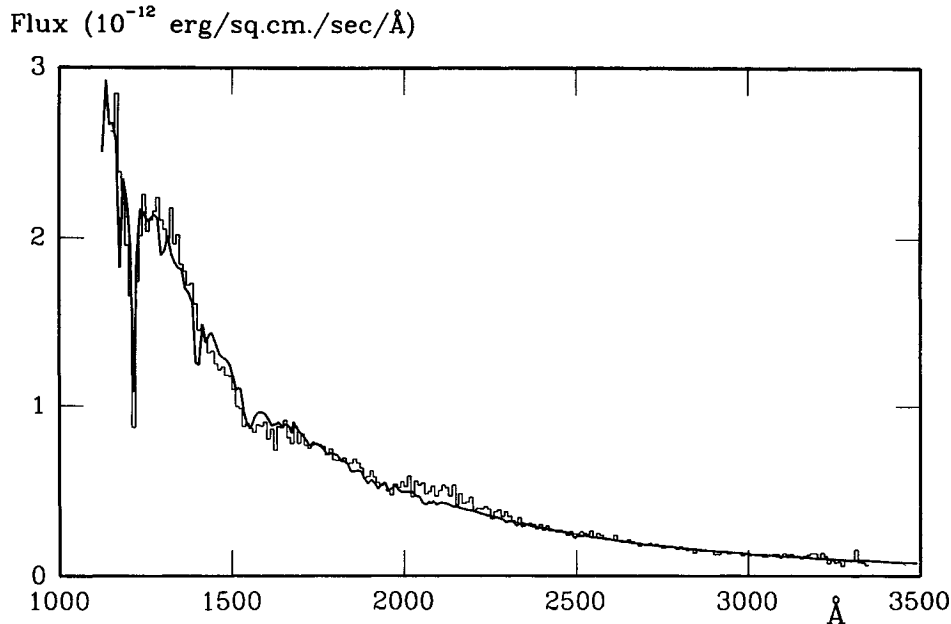


Figure 6. Merged *IUE* LWP and SWP spectrograms (plotted in histogram form) compared to the model spectrum (heavy line) computed with $E(B - V) = 0.05$, $\log g = 6.0$ and $T_{\text{eff}} = 33\,000$ K. The original *IUE* spectrograms have been averaged in 10-Å ‘bins’. The strongest feature in the model is Lyman α (1216 Å); also visible in the model are C III (1175 Å) and Si IV (1404 Å).

trograms, the Paper VI method was simplified by representing the optical region with a single V -band flux density ($V = 13.50$) corresponding to the light curve immediately outside primary eclipse. With interpolation across the optical and near-ultraviolet spectrum, the energy distribution of PG 1336 – 018 was computed over the wavelength range from 1150 to 5500 Å. The satisfactory fit obtained justifies the approximations made. As in Paper VI, the Remie & Lamers (1982) iteration, normalized at the V -band flux density, was used for trial fits with assumed reddening values $E(B - V) = 0.00, 0.03$ and 0.05 . A particularly good fit was obtained with $E(B - V) = 0.05$, and it is shown as the heavy line in Fig. 6. Higher values of reddening are ruled out by the appearance of the 2200-Å feature in emission, indicating over-correction of the reddening effects. The adopted value, $E(B - V) = 0.05$, gives a best fit of $T_{\text{eff}} = 33\,000 \pm 3000$ K for $\log g = 6$ models, and an angular radius of $(5.85 \pm 0.35) \times 10^{-12}$ rad. The excess flux observed near 2100 Å (see Fig. 6) is not centred on the 2200-Å feature, and is therefore unlikely to be due to an incorrect $E(B - V)$. The *IUE* result for T_{eff} is in good agreement with the line profile fitting result noted in Section 5.

Note that the adopted model flux (Fig. 6) contains relatively strong absorption features due to C III (1175 Å) and Si IV (1404 Å), but these are undetected in the observed flux. This is consistent with the canonical model of sdB stars where extreme metal-deficiency is believed to be due to gravitational settling.

The angular radius of the sdB star from the fit to the *IUE* data will give the distance of the system if the actual radius is known. In Section 7 it is argued that the radius of the sdB star is $\sim 1.15 \times 10^5$ km. With the angular size and reddening derived above, and an apparent V magnitude of 13.50 (just outside primary eclipse), the distance to PG 1336 – 018 is then 710 ± 50 pc (where the error is determined from the formal error in the angular radius). The corresponding absolute magnitude of the sdB star is $+4.1 \pm 0.2$, consistent

with results found for other sdB stars using similar methods (e.g. Heber 1986).

7 THE BINARY LIGHT CURVE

For HW Vir, Menzies & Marang (1986) determined a radial velocity curve for the primary, $K_1 = 87.9 \pm 4.8$ km s $^{-1}$, and used the light-curve analysis code by Wilson & Devinney (1971) to fit *UBVRI* light curves. Assuming a temperature for the primary (from *UBV* colours) of $T_1 = 26\,000$ K, they derived a secondary temperature, $T_2 = 4500 \pm 500$ K, and relative radii, $r_1 = 0.203$ and $r_2 = 0.207$.

Wood et al. (1993) obtained simultaneous *BVRI* photometry and also used the Wilson–Devinney code to analyse the data. They found a fairly tightly constrained orbital inclination, $i = 80^\circ 6 \pm 0.2^\circ$, a primary temperature $29\,000 \text{ K} < T_1 < 36\,000 \text{ K}$ and a secondary temperature $T_2 \sim 3700$ K, although the secondary contributes so little light to the system directly (apart from the reflected primary light) that T_2 is not well constrained by the light curves. The mass ratio cannot be directly determined because only spectral features from the primary are visible, but other arguments suggest a value in the range 0.28 to 0.34 (Wood et al. 1993). Further experiments with the system parameters led Wood et al. to conclude that better fits to the HW Vir light curves could be obtained with an albedo for the secondary of 1.0 (rather than the ‘expected’ value of 0.5) and limb-darkening coefficients between 0.0 and 0.5 (rather than 1.0). They also find component radii of $R_1 = 0.18 R_\odot$ and $R_2 = 0.19 R_\odot$, in agreement with Menzies & Marang (1986). Assuming a primary mass $M_1 = 0.5 M_\odot$, consistent with typical sdB masses (Saffer et al. 1994), gives a secondary mass of $0.16 M_\odot$, equivalent to a mid/late M star, which conflicts a little with $T_2 \sim 3700$ K, but not seriously, since the secondary temperature is not well known and, in any case, the cool star is substantially hotter on the side facing the primary than would be an isolated star of identical nature.

Hilditch, Harries & Hill (1996) used echelle spectrograms to redetermine the primary velocity curve of HW Vir (finding $K_1 = 83.0 \pm 1.2 \text{ km s}^{-1}$ – in good agreement with Menzies & Marang 1986), and also searched unsuccessfully for spectral features from the secondary. Hilditch et al. remark on the difficulty in fitting HW Vir light curves, in the sense that it seems necessary, irrespective of the analysis code, to use ‘unphysical’ parameters – unit albedos for cool stars, and zero or even negative limb-darkening coefficients (‘limb-brightening’) – to obtain solutions. The situation is confused because the side of the secondary facing the primary may be heated to 10 000–15 000 K above ‘normal’. Hilditch et al. note that it is likely that the current understanding and modelling of stellar atmospheres irradiated by strong ultraviolet fluxes is inadequate to deal with systems such as HW Vir, where a very hot and a very cool star are in such close proximity.

With these caveats in mind, an attempt has been made to model the U , V and R data for PG 1336 – 018 listed in Table 1, using the `BINARY MAKER` package by Bradstreet (1993). The results should be considered to be preliminary, as the light curves were obtained in ‘high-speed’ mode – that is, without local comparison stars. It is possible, therefore, that residual zero-point drifts may be present in the data, and these could affect the analysis. The data from the last five runs listed in Table 1 were phased according to the ephemeris given in Section 4. The data were then averaged in phase bins of 0.02ϕ outside primary eclipse and 0.005ϕ through primary eclipse. Apart from improving the accuracy of individual data points and yielding a smaller number of points to handle, the averaging process smooths out the very obvious pulsation effects. Since the data were obtained in 10-s integrations and the out-of-eclipse phase bins are ~ 3 min wide, a typical data point had 17 or 18 points averaged into it. In the case of the V light curve, where three runs have been added together, there are sometimes over 50 points in the averages. In some phase intervals there are small differences between the different runs (~ 0.01 mag and probably due to the residual zero-point effects noted above), these have generally been included in the average values. The phase-averaged data were then converted to intensity and normalized to a value of unity at phase 0.25 (or 0.75) for comparison with the output light curves modelled by `BINARY MAKER`.

To the novice at binary light-curve analysis, it seems that a fundamental problem is that there are too many variables and, worse, that in such analyses, some of these variables are correlated so that, for example, varying the inclination of the orbit, the radii of the stars and the limb-darkening coefficients can all have somewhat similar effects on the emergent light curve. Where parameters cannot be determined (e.g., if the spectrum of only one component is detectable – as with PG 1336 – 018), a range of solutions will be possible. It is useful, therefore, if other sources can be used to help fix some of the parameters, or at least to check on the consistency of solutions.

In the case of PG 1336 – 018, it is probably safe to assume that the orbit is circular and that stellar rotation is synchronized with the orbit, as the time-scales for both circularization and synchronization are only a decade or two in such a close system (Zahn 1977; Kilkeny et al. 1994). The most obvious ‘fixable’ parameter is the temperature of the sdB

primary, which was determined to be $T_1 = 33\,000 \text{ K}$ in the line profile analysis presented in Section 5 and the *IUE* data analysis in Section 6. The line profile analysis determined the surface gravity of the sdB to be $\log g = 5.7$. Using Newtonian mechanics, and assuming the mass of the sdB star to be $0.5 M_\odot$ (Saffer et al. 1994), the radius of the sdB star is $R_1 \sim 1.15 \times 10^5 \text{ km}$, or $0.165 R_\odot$. Some preliminary light-curve solutions showed that the relative radii of the two components are fairly tightly constrained at 20 per cent of their separation ($r_1 = 0.19$, $r_2 = 0.20$). The inferred radius of the secondary would then be $R_2 \sim 0.175 R_\odot$. The large reflection effect shows that the secondary is cool; the small radius dictates that it must be a mid/late M dwarf if it is a ‘normal’ star. Models of late-type stars by Dorman, Nelson & Chau (1989) with radii near $0.175 R_\odot$ have temperatures of $\sim 3200 \text{ K}$ and masses of $0.15 M_\odot$. The mass ratio of the system, $q = M_2/M_1$, is 0.3 in this case.

Hilditch et al. (1996) have noted that, although there is good evidence for sdB masses being close to $0.5 M_\odot$ (Saffer et al. 1994), there is at least one example of a smaller mass, namely the sdB binary, HD 185510, for which Jeffery, Simon & Lloyd Evans (1992) obtain a mass in the range 0.31 to $0.37 M_\odot$. If the calculation in the previous paragraph is repeated with the sdB mass taken to be $0.33 M_\odot$, then the following values are obtained: $R_1 = 0.135 R_\odot$, $R_2 = 0.14 R_\odot$, $T_2 \sim 3000 \text{ K}$, $M_2 = 0.12 M_\odot$, and the mass ratio is $q = 0.36$.

The ranges of secondary mass and temperature obtained in these two examples are consistent with an M dwarf star of type $\sim M4$ to $M5$ (see, e.g., Baraffe & Chabrier 1996).

Accepting the above assumptions and derivations (circular orbits; $r_1 = 0.19$, $r_2 = 0.20$), primary masses of 0.5 and $0.33 M_\odot$ give the component separation as 5.51×10^5 and $4.88 \times 10^5 \text{ km}$ respectively (by Kepler’s third law). The corresponding mass ratios ($q = 0.3$ and 0.36) then give the radius of the primary orbit as 1.27×10^5 and $1.29 \times 10^5 \text{ km}$, and the known period (0.101 0174 d) results in orbital velocities of 91 and 93 km s^{-1} respectively – in broad agreement with the velocity semi-amplitudes given in Table 3 (within the spread of the data, at least). The orbital inclination is $i \sim 81^\circ$, which reduces the orbital velocity by only ~ 1 per cent to yield the projected semi-amplitude. The parameters derived above are thus consistent with the observations and are also internally consistent.

To model the observed light curves, the following parameters were set: the mass ratio, $q = 0.3$; the temperatures, $T_1 = 33\,000 \text{ K}$ and $T_2 = 3000 \text{ K}$; the gravity-darkening exponent was assumed to be 1.0 for the primary (von Zeipel 1924) and 0.32 for the (presumably) convective secondary (Lucy 1967); the albedo of the primary was assumed to be 1.0; and the limb-darkening coefficients were interpolated from table 1 of Al Naimiy (1978). With these values fixed, `BINARY MAKER` was used to generate model light curves with varying values of the relative radii (r_1 , r_2), orbital inclination (i), and albedo and limb-darkening coefficients of the secondary. Modelling was first done for the U data (as this had seemed easiest in the preliminary modelling), then V and finally R . The sequence was iterated until consistent results were achieved. The relative radii and orbital inclination are fairly tightly constrained by the depth and width of the eclipses, and were set to $i = 81^\circ$, $r_1 = 0.19$ and $r_2 = 0.205$ early in the process. Although conventional starting values for the albedo and limb-darkening coefficients for a cool star

were assumed (0.5 and ~ 1.0 , respectively; e.g. Ruciński 1969; Al Naimiy 1978), it rapidly became clear that these values could not match the observations. It appeared necessary to use values near zero for the limb-darkening coefficients for U and V , and values near to unity for the reflection effect at all three passbands.

With a consistent set of values for the binary parameters, experiments were made by keeping all parameters except one fixed and varying a single parameter to get a measure of the range over which that parameter could be varied and still maintain a fair fit to the data. This perhaps gives conservative values of the errors involved, but it is in any case difficult to assess errors, since it is clear that varying one parameter away from optimum can be compensated (in a formal error sense) by varying a different parameter – the result might still have low error, but be a worse approximation to what passes for reality.

The ‘best’ solution has parameters as follows:

$q = 0.3$ (assumed)
 $i = 81^\circ \pm 0.5$
 $T_1 = 33\,000 \pm 2000$ K (assumed)
 $T_2 = 3000 \pm 1000$ K (assumed)
 $r_1 = 0.19 \pm 0.01$
 $r_2 = 0.205 \pm 0.01$
 limb-darkening (1) 0.30, 0.25, 0.20 (UVR) (assumed)
 limb-darkening (2) 0.0, 0.0, 1.0 (UVR)
 albedo (1) 1.0, 1.0, 1.0 (UVR) (assumed)
 albedo (2) 1.0, 0.9, 1.1 (UVR),

and the model light curves are compared to the mean light curves in Fig. 7. Estimated uncertainties in the limb-darkening coefficients and albedos of the secondary are ~ 0.2 and ~ 0.1 respectively, but note that it has been necessary to force the limb-darkening coefficients to zero at U and V , and all the albedos to ~ 1.0 . In the case of the R passband, the ‘best’ fit requires a limb-darkening coefficient near unity and an albedo greater than 1.0 to get close to the observed reflection effect. No really satisfactory fit to R was obtained with the parameters used.

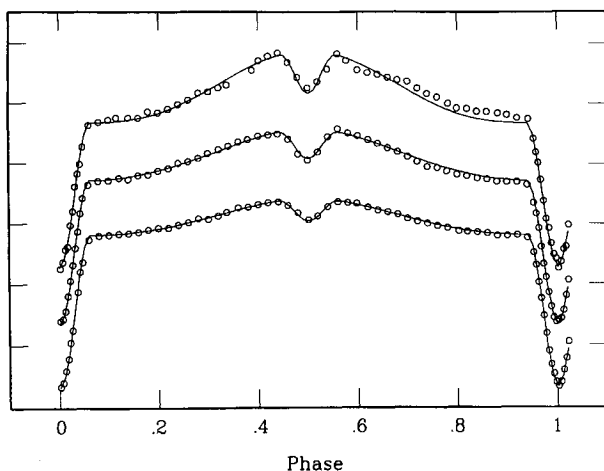


Figure 7. Phase-binned data points (open circles) from the last five runs listed in Table 1. The circle radii are 1 per cent of unit intensity. From the top downwards, the light curves are R , V and U . The continuous lines represent the solutions discussed in Section 6. The abscissa is orbital phase, and the ordinate is intensity normalized to unity at phase 0.25. The ordinate carets are separated by 0.2, or 20 per cent of the intensity at phase 0.25.

Because the secondary only effectively contributes to the total light by the reflection effect, it is possible to vary T_2 by a large relative amount and hardly affect the modelled light curve.

In Fig. 7 the radii of the small circles representing the mean data are 1 per cent of the unit intensity. From the figure it can be seen that for the U passband, the model matches the data to better than 1 per cent for essentially the whole orbit. At V , there appear to be systematic deviations of about 1 per cent (see especially $0.7 < \text{phase} < 0.9$) and at R , deviations up to about 3 per cent. Given that these deviations are asymmetric with respect to phase 0.5, it is quite possible that the deviations arise from small ‘drifts’ in the ‘high-speed’ data which are uncontrolled (i.e., not differential). Drifts of ~ 0.01 – 0.03 mag are not uncommon over a few hours, even at a good site in apparently good conditions (a similar effect can be seen in the Wood et al. 1993 data – see their fig. 2). This is, after all, one of the reasons why we bother to observe standards. It is also possible that the smoothing effect of phase-binning the data might introduce small systematic effects, although comparison of the smoothed data with the original data suggests that this should have little effect.

Finally, some models were produced with variation of parameters which had previously been held fixed, and it is worth mentioning a couple of these. First, it appeared possible to obtain comparable, or even better, fits to the photometry with a mass ratio, $q = 1$ (and consequent changes to some of the other parameters). If $q = 1$ and if it is accepted that sdB stars have masses close to $0.5 M_\odot$ (e.g., Saffer et al. 1994), then the mass of the secondary must also be $0.5 M_\odot$, corresponding to a star of type $\sim M2$ and $T_{\text{eff}} = 3600$ K – within the limits noted above (although the radius would then be rather large at $\sim 0.5 R_\odot$). However, if $q = 1$, the observed radial velocity semi-amplitude of the sdB star would be $K_1 \sim 200 \text{ km s}^{-1}$, which seems completely ruled out by Fig. 5. From the light curve alone, larger mass ratios cannot be ruled out but, assuming the sdB to have a mass near $0.5 M_\odot$ and that the velocity curve is not grossly in error, q values much in excess of the assumed 0.3 would seem to be excluded. Secondly, in an analysis of the eclipsing system AA Dor, Kilkenny, Penfold & Hilditch (1979) found it necessary to use very small (0.03) limb-darkening parameters for the sdOB primary, in order to fit in detail the shape of primary eclipse. Models of PG 1336 – 018 with primary limb-darkening coefficients of zero certainly seem reasonable, but the effect of changing these parameters is on primary ingress and egress, which are not nearly as well defined here as for AA Dor. Indeed, it might be extremely difficult to derive limb-darkening coefficients from the shape of the primary eclipse of PG 1336 – 018 if there are residual pulsation effects present, unless these could be removed by precise pulsation modelling.

In all the models considered, both stars were well within their Roche lobes, so there is no reason to expect evidence for mass-loss or mass-transfer by Roche-lobe overflow.

8 SUMMARY AND DISCUSSION

It has been shown that PG 1336 – 018 is a short-period eclipsing binary, very similar photometrically to HW Vir, with the additional factor that the sdB primary is a rapidly

Table 4. Comparison of HW Vir and PG 1336 – 018.

Parameter	HW Vir	PG1336-018
Orbital period (day)	0.1167196	0.1010174
Orbital period change	decrease	not yet known
Orbital inclination (°)	80.6±0.2	81±0.5
mass ratio	~0.3	~0.3
K_1 (km/s)	83.0±1.2	78±3
T_1 (K)	33000±700	33000±2000
T_2 (K)	3700±700	3000±1000
r_1	0.205±0.003	0.19±0.01
r_2	0.211±0.004	0.205±0.01
M_1 (M_\odot) (assumed)	0.54	0.5
M_2 (M_\odot)	0.16	0.15

pulsating star of the recently discovered EC 14026 class. Frequency analyses of continuous data in various passbands reveals pulsation frequencies at 5.435 mHz (184.0 s) and 7.076 mHz (141.3 s) with a suggestion of other frequencies between about 5 and 8 mHz having very small amplitude (≤ 0.003 mag). The period of the orbit, 0.1010174 d, is amongst the shortest known for detached systems, and it is probable that any orbital period change will be detectable in two or three more years of observation – if the system is behaving in the same way as HW Vir (although recent unpublished results for HW Vir indicate that the rate of period change is not constant and may exhibit ‘stand-stills’).

Preliminary analyses of the U , V and R light curves of PG 1336 – 018 have been based on the derivation of T_{eff} and $\log g$ from spectroscopy and the assumption that the sdB mass is $0.5 M_\odot$. The mass and surface gravity fix the primary radius, and the light curve shows that the primary and secondary radii are very similar, which reveals the nature of the secondary star, a mid-M dwarf. The mass ratio is defined thus, and supported by the radial velocity curve of the primary. Although the approach has been somewhat different to that of Wood et al. (1993) in their analysis of HW Vir, it is found that the temperatures, radii and masses of the primary and secondary star in each system are closely similar. The assumptions made in this paper have required values for the albedos and limb-darkening coefficients of the secondary star which are also similar to those derived for HW Vir, although the physical meaning of essentially zero limb-darkening and reflection effects equal to, or greater than, unity remains unclear (Hilditch et al. 1996).

In Table 4 is given a comparison of the features of the HW Vir and PG 1336 – 018 systems. The close similarity is striking; even the orbital inclination is amusingly similar (not being cosmologists, we attempt to draw no statistical conclusions, but rely on the existence of coincidence to explain this). Whilst two stars may form a class, they hardly form a significant sample; none the less, the existence of HW Vir and PG 1336 – 018 indicates that there must be a mechanism for producing such systems. Certainly, given their present configuration, they will have undergone a ‘common-envelope’ phase, but the detailed similarity suggests that the mechanism must have fairly tight constraints on its end-product. Clearly, it would be of great interest if further such systems could be found.

ACKNOWLEDGMENTS

We are grateful to Dr R. S. Stobie for two high-speed photometry runs, and thank an anonymous referee for positive comments.

REFERENCES

- Abt H. A., Biggs E. S., 1972, *Bibliography of Stellar Radial Velocities*. Kitt Peak National Observatory
- Al Naimiy H. M., 1978, *Ap&SS*, 53, 181
- Baraffe I., Chabrier G., 1996, *ApJ*, 461, L51
- Bevington P. R., 1969, *Data reduction and Error Analysis for the Physical Sciences*. McGraw-Hill, New York. p. 140
- Bradstreet D. H., 1993, *BINARY MAKER 2.0*. Contact Software
- Charpinet S., Fontaine G., Brassard P., Chayer P., Rogers F. J., Iglesias C. A., Dorman B., 1998, *ApJ*, in press
- Deeming T. J., 1975, *Ap&SS*, 36, 137
- Dorman B., Nelson L. A., Chau L. Y., 1989, *ApJ*, 342, 1003
- Green R. F., Schmidt M., Liebert J., 1986, *ApJS*, 61, 305
- Hilditch R. W., Harries T. J., Hill G., 1996, *MNRAS*, 279, 1380
- Heber U., 1986, *A&A*, 155, 33
- Jeffery C. S., Simon T., Lloyd Evans T., 1992, *MNRAS*, 258, 64
- Kilkenny D., Penfold J. E., Hilditch R. W., 1979, *MNRAS*, 187, 1
- Kilkenny D., Heber U., Drilling J. S., 1988, *SAAO Circ.* 12, 1
- Kilkenny D., Marang F., Menzies J. W., 1994, *MNRAS*, 267, 535
- Kilkenny D., Koen C., O’Donoghue D., Stobie R. S., 1997a, *MNRAS*, 285, 640 (Paper I)
- Kilkenny D., O’Donoghue D., Koen C., Stobie R. S., Chen A., 1997b, *MNRAS*, 287, 867
- Koen C., Kilkenny D., O’Donoghue D., van Wyk F., Stobie R. S., 1997, *MNRAS*, 285, 645 (Paper II)
- Kurtz D. W., 1985, *MNRAS*, 213, 773
- Lucy L. B., 1967, *Z. Astrophys.*, 65, 89
- Lynas-Gray A. E., Kilkenny D., Skillen I., Jeffery C. S., 1986, in Hunger K., Schönberner D., Rao K., eds, *Proc. IAU Colloq. 87, Hydrogen-deficient stars and related objects*. Reidel, Dordrecht, p. 87
- Menzies J. W., Marang F., 1986, in Hearnshaw J. B., Cottrell P. L., eds, *Proc. IAU Symp. 118, Instrumentation and Programmes for Small Telescopes*. Reidel, Dordrecht, p. 305
- Nichols J. S., Linsky J. L., 1996, *AJ*, 111, 517
- O’Donoghue D., Koen C., Kilkenny D., 1996, *MNRAS*, 278, 1075
- O’Donoghue D., Lynas-Gray A. E., Kilkenny D., Stobie R. S., Koen C., 1997, *MNRAS*, 285, 657 (Paper IV)
- O’Donoghue D. et al., 1998a, *MNRAS*, 296, 296
- O’Donoghue D., Koen C., Lynas-Gray A. E., Kilkenny D., van Wyk F., 1998b, *MNRAS*, 296, 306
- Patterson J., 1984, *ApJS*, 54, 443
- Remie H., Lamers H. J. G. L. M., 1982, *A&A*, 105, 85
- Ritter H., 1987, *A&AS*, 70, 335
- Ruciński S. M., 1969, *Acta Astron.*, 19, 245
- Saffer R. A., Bergeron J., Koester D., Liebert J., 1994, *ApJ*, 432, 351
- Stobie R. S., Kawaler S. D., Kilkenny D., O’Donoghue D., Koen C., 1997a, *MNRAS*, 285, 651 (Paper III)
- Stobie R. S. et al., 1997b, *MNRAS*, 287, 848
- von Zeipel H., 1924, *MNRAS*, 84, 665
- Wesemael F., Fontaine G., Bergeron P., Lamontagne R., Green R. F., 1992, *AJ*, 104, 203
- Wilson R. E., Devinney E. J., 1971, *ApJ*, 166, 605
- Wood J. H., Zhang E.-H., Robinson E. L., 1993, *MNRAS*, 261, 103
- Zahn J.-P., 1977, *A&A*, 57, 383